ISSN 1819-7124, Neurochemical Journal, 2018, Vol. 12, No. 4, pp. 305–310. © Pleiades Publishing, Ltd., 2018.
Original Russian Text © V.V. Kravtsova, N.A. Timonina, G.F. Zakir'yanova, A.V. Sokolova, V.M. Mikhailov, A.L. Zefirov, I.I. Krivoi, 2018, published in Neirokhimiya, 2018, Vol. 35, No. 4, pp. 301–307.

EXPERIMENTAL ARTICLES

# The Structural and Functional Characteristics of the Motor End Plates of Dysferlin-Deficient Mice

**V. V. Kravtsova[a], N. A. Timonina[a], G. F. Zakir'yanova[b], A. V. Sokolova[c], V. M. Mikhailov[c], A. L. Zefirov[d], and I. I. Krivoi[a, 1]**

[a] *St. Petersburg State University, St. Petersburg, Russia*
[b] *Kazan Institute of Biochemistry and Biophysics, Federal Research Center Kazan Scientific Center, Russian Academy of Sciences, Kazan, Russia*
[c] *Institute of Cytology, Russian Academy of Sciences, St. Petersburg, Russia*
[d] *Kazan State Medical University, Kazan, Russia*

Received April 9, 2018

**Abstract**—The molecular mechanisms that underlie neuromuscular junction plasticity are complex and remain to be fully elucidated. Experimental models of various forms of impaired motor activity may be promising for their study. The dysferlin protein plays a key role in the multimolecular complex, which maintains sarcolemma integrity and the functioning of skeletal muscle cells. We studied the structural and functional characteristics of the diaphragm muscle motor end plates of dysferlin-deficient Bla/J mice (a model of dysferlinopathy), dystrophin-deficient mdx mice (a model of Duchenne muscular dystrophy), and control C57Bl/6 mice. Increased end plate fragmentation and a decrease in the area of individual fragments were observed in mdx mice and absent in Bla/J mice, which indicates a difference in these models of myodystrophy from these characteristics. However, end plates of both mice lines were characterized by a decrease in the density of distribution of nicotinic acetylcholine receptors, as well as by membrane depolarization, presumably, due to altered functional interaction between the α2 isoform of Na,K-ATPase and the nicotinic acetylcholine receptors.

*Keywords:* skeletal muscle, motor endplate, nicotinic acetylcholine receptors, dysferlin, dysferlinopathy

**DOI:** 10.1134/S1819712418040049

## INTRODUCTION

The plasticity of synapses and the nervous system as a whole is one of the most important issues in modern neurophysiology. The cholinergic neuromuscular synapse remains a traditional model in this field. Tigran Mel'kumovich Turpaev, Academician of the Russian Academy of Sciences, made an outstanding contribution to the studies on this model by showing that the action of acetylcholine, a mediator of the nervous system, is mediated by protein molecules—postsynaptic cholinergic receptors [1, 2]. The motor end plate of the neuromuscular synapse of vertebrates is a highly specialized area of the sarcolemma that lies just below the motor nerve terminal and is characterized by an exceptionally high density of nicotinic acetylcholine receptors [3, 4]. After the release of a quanta of acetylcholine from the nerve terminal the mediator molecules interact with nicotinic acetylcholine receptors, which leads to the generation of a local end plate potential. The process of transformation of the local potential of the end plate into a propagating action potential is one of the key stages on which depends not only the efficiency of the neuromuscular transmission but also its plasticity [3, 4].

The most important factors of reliability and plasticity of neuromuscular transmission are the structural organization of the end plate and its electrogenesis. The ultrastructure of the end plate is highly dependent on motor activity. A decrease in motor activity during aging [5], in muscular pathologies [6, 7], as well as under conditions of functional relief [8], is accompanied by a change in the area of the end plates and increased fragmentation in the distribution of nicotinic acetylcholine receptors. Even a short-term motor discharge decreases the level of membrane cholesterol [9] and the electrogenic activity of the α2 isoform of Na,K-ATPase [10], the factors that are important for maintenance of the resting membrane potential (RMP) in the region of the end plate [11].

The molecular mechanisms that underlie the plasticity of the end plate structure are very complex and largely unclear [12–15]. The experimental models of various forms of disturbances in motor activity may be promising for further studies on the plasticity mecha-

[1] Corresponding author; address: Universitetskaya nab. 7/9, St. Petersburg, 199034 Russia; email: iikrivoi@gmail.com.

nisms of the end plate. These disorders include dysferlinopathies that develop with a deficiency of dysferlin, which is a key protein of the multimolecular complex responsible for the restoration of the integrity of the sarcolemma [16, 17]. The molecular mechanism of maintenance of the integrity of the plasma membrane is of fundamental importance for the normal functioning of skeletal muscle cells. The motor activity can cause microdamage of the sarcolemma with subsequent entry of external $Ca^{2+}$ at these sites, disruption of excitation–contraction coupling, activation of a number of $Ca^{2+}$-dependent cascades, including $Ca^{2+}$-dependent proteolysis and oxidative stress. Taken together, this will cause further damage to the muscle fiber, inflammation, necrosis, and myopathy [16, 17]. According to modern ideas, the integrity of the plasma membrane is restored via the $Ca^{2+}$-dependent mechanism of fusion of membrane-bound intracellular vesicles with the sarcolemma at the sites of its damage and the key protein that coordinates this mechanism is dysferlin. In mice with deficient dysferlin synthesis, progressive muscular dystrophy is observed and humans with mutations in the dysferlin gene have so-called dysferlinopathies [17]. Thus, dysferlinopathies differ fundamentally in their mechanism from Duchenne myodystrophy caused by loss of integrity between the cytoskeleton, the dystrophin–glycoprotein complex, and extracellular matrix proteins due to decreased synthesis of dystrophin protein [18].

The mice of the mdx line, which are the laboratory model of Duchenne myodystrophy [18], have an altered area of the end plates and their defragmentation [6, 7], as well as the depolarization of the sarcolemma [19, 20]. There is no similar information on animals with disturbed synthesis of dysferlin in the literature. In this study, the distribution of nicotinic acetylcholine receptors, the degree of fragmentation and the area of the end plates, as well as the RMP values in the diaphragm muscle of Bla/J mice (one of the models of dysferlinopathy [21, 22]) were compared with mdx mice and C57Bl/6.

## MATERIALS AND METHODS

This study was performed with isolated neuromuscular preparations of the diaphragm of male C57Bl/6, Bla/J, and mdx mice (all aged 5–7 months).

Immediately after isolation, a strip of semi-diaphragm with a nerve segment was placed in an experimental chamber with a physiological solution of the following composition (in mM): NaCl, 137; KCl, 5; $CaCl_2$, 2; $MgCl_2$, 2; $NaHCO_3$, 24; $NaH_2PO_4$, 1; glucose, 11; pH 7.4. The solution was constantly aerated with carbogen (95% $O_2$ + 5% $CO_2$). The determination of the localization of nicotinic acetylcholine receptors was performed at room temperature at approximately 22°C using labeled α-bungarotoxin (α-BTX) (tetramethylrhodamine-bungarotoxin, Biotium, United States) as described previously [9]. To obtain the images, a Leica TCS SP5 confocal system with a 63× lens and a numerical aperture of 1.30 was used; image processing was performed using the ImageJ program. In experiments with the RMP recording, a flowing aerated carbogen solution with a temperature of 28°C was used. Before the start of the experiment, the muscles were kept under these conditions for 60 minutes. The RMP value was recorded intracellularly using glass microelectrodes with internal capillaries (BF150-110-10, Sutter Instrument, Co., United States) made on a Sutter P-97 puller (United States) as previously described [10].

Sigma's chemical reagents were used. Statistical analysis was performed using Origin software (ORIGIN Pro 8 software) and the Student and ANOVA tests. The cumulative curves were analyzed using the Kolmogorov–Smirnov test (GraphPad Prism 7 software). The text, table, and figures show the mean values and their errors ($m \pm$ S.E.).

## RESULTS AND DISCUSSION

Typical images of the distribution of nicotinic acetylcholine receptors in the end plates of mice of different lines are shown in Fig. 1 (a, b, and c). It is well known that nicotinic acetylcholine receptors within the end plate are distributed as separate fragments [5, 7]. In Bla/J mice, the number of fragments per end plate averaged 2.6 ± 0.1 (210 end plates, 12 muscles, and 8 mice), which did not differ from 2.4 ± 0.1 (233 end plates, 27 muscles, and 16 mice) in control C57Bl/6 mice. The corresponding cumulative curves also did not differ (Fig. 1d). The mdx mice showed a significant ($p < 0.01$) increase in the number of fragments on average to 6.1 ± 0.3 (121 end plates, 18 muscles, and 12 mice) and a corresponding shift ($p < 0.01$) of the cumulative curve toward higher values compared to C57Bl/6 and Bla/J mice (Fig. 1d).

The distribution of the areas of individual fragments in the control muscles was best approximated by 3 normal distributions and indicated the predominance of relatively large fragments with an average area of 143 ± 7 μm$^2$ (Fig. 1f). In Bla/J mice, the distribution of the areas of the fragments and the corresponding cumulative curves did not differ significantly from the control curves; we observed only a tendency to a shift of the peak of the distribution of the areas of large fragments to lower values (mean area 119 ± 8 μm$^2$) (Figs. 1e and 1g). In mdx mice, a significant ($p < 0.01$) peak shift in the distribution of areas of large fragments was observed in the region of lower values (average area 50 ± 15 μm$^2$), and relatively small fragments predominated in the distribution (Fig. 1 h). There was also a corresponding significant ($p < 0.01$) shift of the cumulative curve to the left (Fig. 1e).

The total area of each end plate was defined as the sum of the areas of all its fragments. In C57Bl/6,

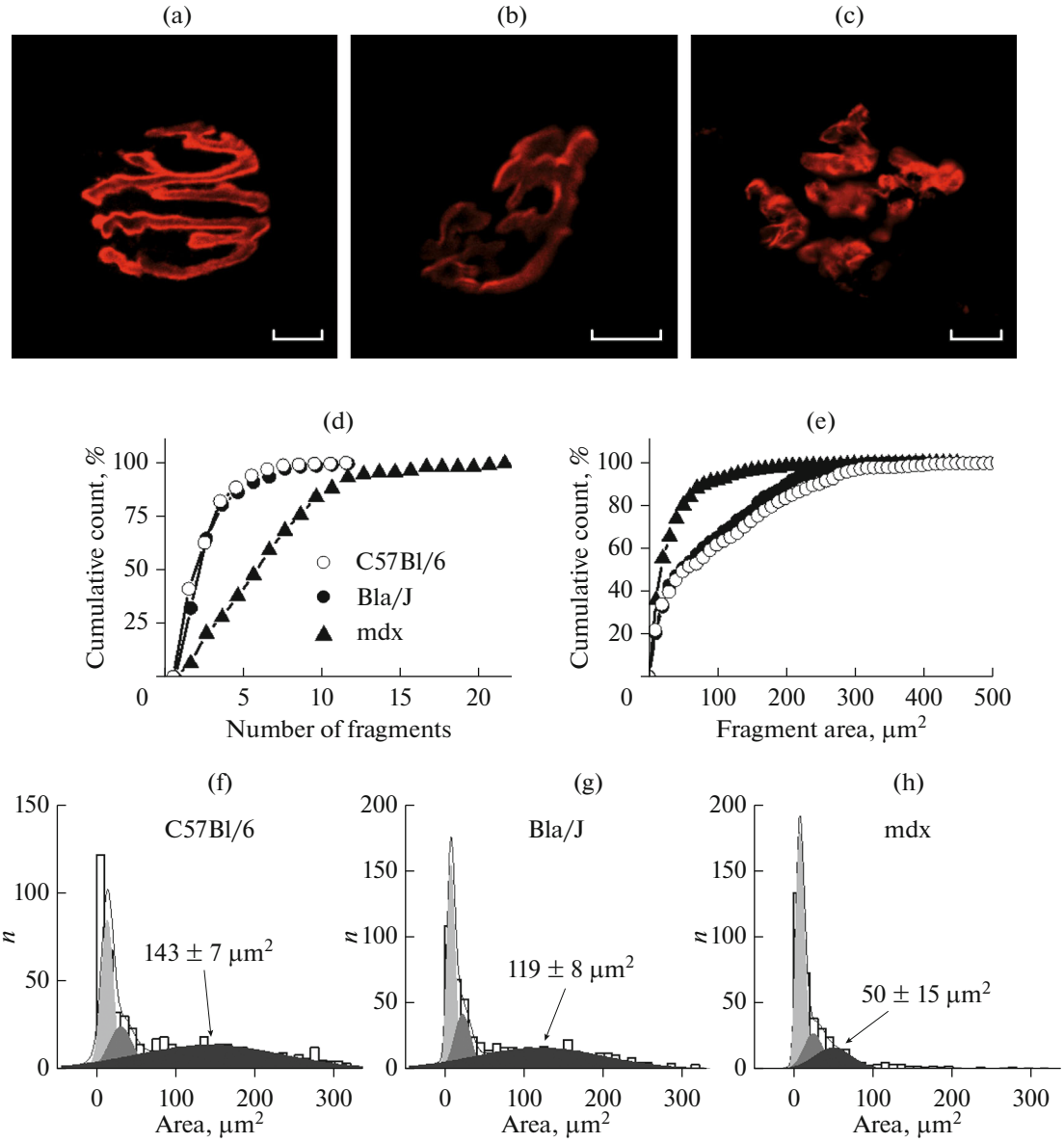


**Fig. 1.** Examples of images of the distribution of nicotinic acetylcholine receptors labeled with α-BTX (red channel), in the end plates of C57Bl/6 (a), Bla/J (b) and mdx (c) mice. Scale: 10 μm. (d and e) are cumulative curves that reflect the distribution of end plates according to the number of fragments contained in them (d) and the areas of individual fragments (e). Histograms of the area distributions of individual fragments of end plates in C57Bl/6 (f), Bla/J (g) and mdx (h) mice. The arrows show the distribution of areas of large fragments (the numbers above the arrows show the average area of large fragments).

Bla/J, and mdx mice, the total area of the end plates averaged 229 ± 6, 205 ± 5, and 212 ± 8 μm$^2$, respectively (Fig. 2a). In the Bla/J and mdx mice, a significant ($p < 0.01$) decrease in the relative fluorescence level of α-BTX per unit area of the end plate was observed at 26 and 33%, respectively (Fig. 2b); the total fluorescence level of α-BTX significantly decreased ($p < 0.001$) throughout the end plate area (Fig. 2c).

It is possible to assume that the decrease in the fluorescence level of α-BTX in Bla/J mice and, in particular, in mdx mice is due, for example, to the defragmentation of the end plates and the lower density of distribution of nicotinic acetylcholine receptors in small fragments. However, analysis of the dependence of the fluorescence level of α-BTX on the area of individual fragments of end plates does not support this assumption (Fig. 3).

In the diaphragm muscles of C57Bl/6 mice, the RMP value in the postsynaptic region of the membrane was 4.1 ± 0.5 mV ($p < 0.01$) more negative in comparison with the extrasynaptic region (Table 1). This is a well-known effect of local hyperpolarization of the postsynaptic membrane due to the higher elec-

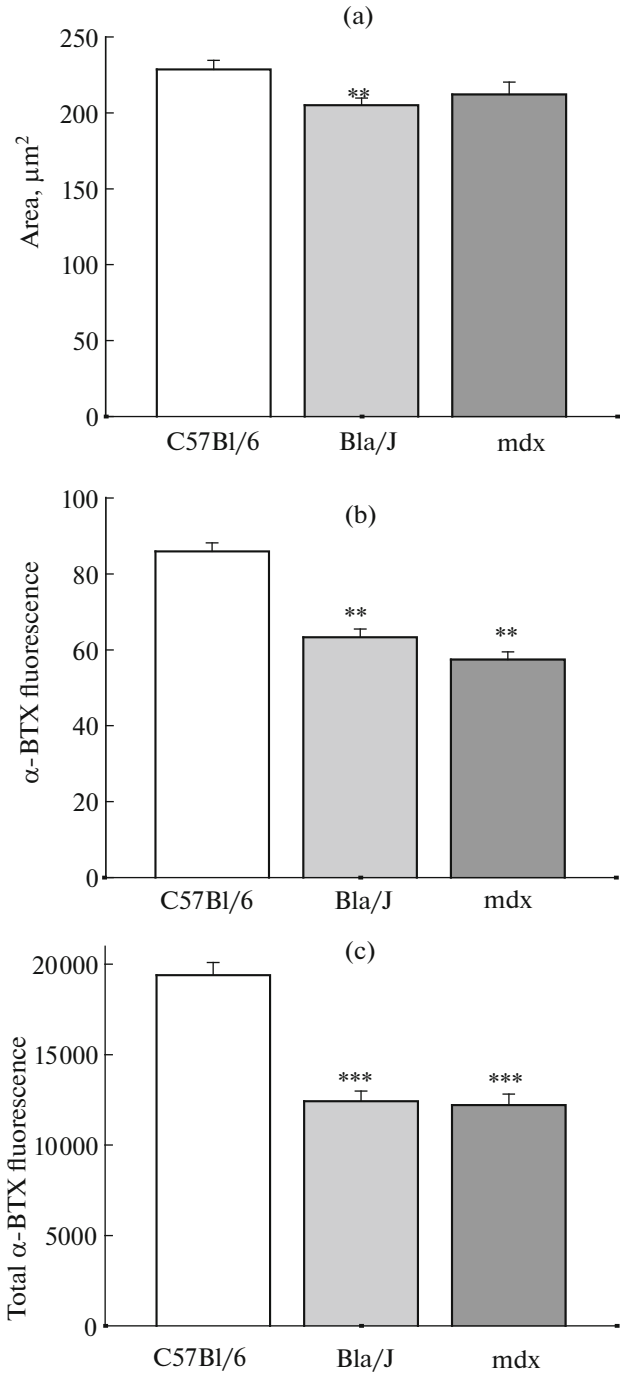


**Fig. 2.** (a) The total area of the end plates; (b) fluorescence intensity of α-BTX per unit area; (c) fluorescence intensity of α-BTX corresponding to the total area of end plates in C57Bl/6, Bla/J, and mdx mice. ** and ***, significant differences in comparison with the control (C57Bl/6), $p < 0.01$ and $p < 0.001$.

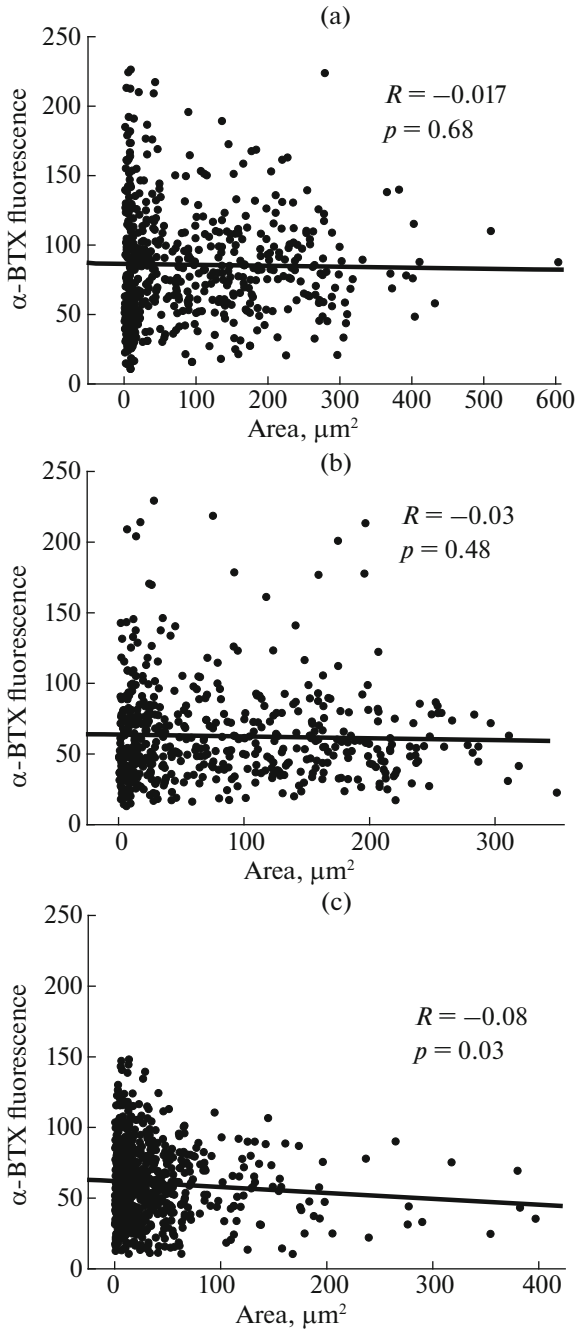


**Fig. 3.** The dependence of the relative fluorescence level of α-BTX on the area of individual fragments of end plates of C57Bl/6 (a), Bla/J (b), and mdx (c) mice.

trogenic activity of the α2-isoform of Na,K-ATPase due to its functional interaction with nicotinic acetylcholine receptors [23, 24]. In the muscles of mdx mice, both regions of the sarcolemma were depolarized to the level of approximately –74 mV; there was no local hyperpolarization of the postsynaptic membrane (Table 1). In the muscles of Bla/J mice, depolarization of both regions of the sarcolemma was also observed in comparison with C57Bl/6 mice; however, it was not as strong as in mdx mice and local hyperpolarization of the postsynaptic membrane was also not observed (Table 1).

**Table 1.** The RMP values in different regions of the muscle fibers of the diaphragm of C57Bl/6, Bla/J, and mdx mice. ** Significant difference compared to the corresponding region of the membrane in C57Bl/6 mice (control), $p < 0.01$. Numbers in parentheses are the number of measurements of RMP

| Mice line | C57Bl/6 | Bla/J | mdx |
|---|---|---|---|
| Postsynaptic region | −82.1 ± 0.3 mV (333) | −76.3 ± 0.8** mV (89) | −74.2 ± 0.5** mV (212) |
| Extrasynaptic region | −78.0 ± 0.3 mV (363) | −74.8 ± 0.6** mV (110) | −73.6 ± 0.4** mV (229) |
| Number of muscles | 13 | 4 | 11 |

Our analysis showed that the degree of fragmentation of the end plates of the diaphragm muscle of mdx mice is significantly higher compared to the control mice C57Bl/6, which corresponds to other data [7]. However, this parameter of the end plates in Bla/J mice did not differ from the control. The total area of the end plates in Bla/J mice was only slightly (~10%) but significantly ($p < 0.01$) lower than the control. The mdx mice did not differ in this indicator from the control mice.

In both lines of Bla/J and mdx mice, a significant decrease in the relative fluorescence of α-BTX per unit area was found, which may reflect a decrease in the density of distribution of nicotinic acetylcholine receptors in the membrane whose mechanism remains unclear. It is possible that in mdx mice with a deficiency of cytoskeleton protein dystrophin this decrease is due to the fact that dystrophin and the protein complex associated with it are necessary for maturation and stabilization of clusters of nicotinic acetylcholine receptors in the end plate [25]. Another factor may be autophagy, which is involved in the regulation of the turnover of nicotinic acetylcholine receptors and the structure of the neuromuscular junction [26]. The weakening of the processes of autophagy leads to a degeneration of the neuromuscular junction [5]. Conversely, an increase in autophagy counteracts manifestations of myodystrophic nature in mdx mice [27]. The explanation of the decrease in the density of nicotinic acetylcholine receptors in Bla/J mice is not yet known.

In mdx mice, we observed a general decrease in the electrogenesis of muscle fibers, which is typical of these animals and is primarily due to damage to the sarcolemma due to the absence of the dystrophin cytoskeletal protein. Necrotic sarcolemma damage was also observed with a deficiency of dysferlin [28], which is responsible for the restoration of the plasma membrane integrity. An important reason for the depolarization of sarcolemma in mdx mice may also be a decrease in the electrogenic activity of Na,K-ATPase [20]. For mice with dysferlin deficiency there is no data on muscle electrogenesis and the functioning of Na,K-ATPase in these animals.

## CONCLUSIONS

The study showed that, unlike mdx mice (a model of Duchenne muscular dystrophy), there were no disturbances in the structure of end plates in Bla/J mice (a model of dysferlinopathy). These data further emphasize the difference in these models of muscle pathology [29]. However, we also found common features: both Bla/J and mdx mice had a decrease in the density of distribution of nicotinic acetylcholine receptors in the membrane and depolarization of the sarcolemma. However, not only was the electrogenesis of muscle fibers reduced but there was also no local hyperpolarization of the postsynaptic membrane, which is characteristic of C57Bl/6 mice. Local hyperpolarization is a result of higher electrogenic activity of the α2 isoform of Na,K-ATPase due to its functional interaction with nicotinic acetylcholine receptors [23, 24]; therefore, the absence of this hyperpolarization may indirectly reflect disruption of this mechanism of maintenance of postsynaptic electrogenesis in Bla/J and mdx mice.

## ACKNOWLEDGMENTS

The authors are grateful to the Research Center for Molecular and Cell Technologies of the St. Petersburg State University and personally to N.A. Kostin for help with confocal microscopy.

## COMPLIANCE WITH ETHICAL STANDARDS

*Funding.* This work was supported by the Russian Science Foundation, project no. 18-15-00043.

*Conflict of Interest.* The authors declared no conflicts of interest.

*Ethical statement.* The conditions of keeping animals and working with them corresponded to the norms of international and Russian legislation.

*Informed consent.* This article does not contain any studies with human participants performed by any of the authors.

## REFERENCES

1. Turpaev, T.M. and Putintseva, T.G., *Usp. Fiziol. Nauk*, 1974, vol. 5, no. 1, pp. 17–47.
2. Turpaev, T.M. and Sakharov, D.A., *Zhurn. Evolyuts. Biokhim*, 1967, vol. 3, no. 5, pp. 482–488.
3. Wood, S.J. and Slater, C.R., *Prog. Neurobiol.*, 2001, vol. 64, pp. 393–429.
4. Ruff, R.L., *Muscle Nerve*, 2011, vol. 44, pp. 854–861.

5. Carnio, S., LoVerso, F., Baraibar, M.A., Longa, E., Khan, M.M., Maffei, M., Reischl, M., Canepari, M., Loefler, S., Kern, H., Blaauw, B., Friguet, B., Bottinelli, R., Rudolf, R., and Sandri, M., 2014, *Cell Rep.*, vol. 8, pp. 1509–1521.
6. Sokolova, A.V., Zenin, V.V., and Mikhailov, V.M., *Cell. Tissue Biol.*, 2010, vol. 4, pp. 258–266.
7. van der Pijl, E.M., van Putten, M., Niks, E.H., Verschuuren, J.J., Aartsma-Rus, A., and Plomp, J.J., *Eur. J. Neurosci.*, 2016, vol. 43, pp. 1623–1635.
8. Chibalin, A.V., Benziane, B., Zakyrjanova, G.F., Kravtsova, V.V., and Krivoi, I.I., *J. Cell Physiol.*, 2018, vol. 233, pp. 6329–6336.
9. Petrov, A.M., Kravtsova, V.V., Matchkov, V.V., Vasiliev, A.N., Zefirov, A.L., Chibalin, A.V., Heiny, J.A., and Krivoi, I.I., *Am. J. Physiol. Cell. Physiol.*, 2017, vol. 312, pp. C627–C637.
10. Kravtsova, V.V., Petrov, A.M., Matchkov, V.V., Bouzinova, E.V., Vasiliev, A.N., Benziane, B., Zefirov, A.L., Chibalin, A.V., Heiny, J.A., and Krivoi, I.I., *J. Gen. Physiol.*, 2016, vol. 147, pp. 175–188.
11. Kravtsova, V.V., Petrov, A.M., Vasiliev, A.N., Zefirov, A.L., and Krivoi, I.I., *Bull. Exp. Biol. Med.*, 2015, vol. 158, pp. 298–300.
12. Nishimune, H., Stanford, J.A., and Mori, Y., *Muscle Nerve*, 2014, vol. 49, pp. 315–324.
13. Rudolf, R., Khan, M.M., Labeit, S., and Deschenes, M.R., *Front. Aging Neurosci.*, 2014, vol. 6.
14. Tintignac, L.A., Brenner, H.R., and Ruegg, M.A., *Physiol. Rev.*, 2015, vol. 95, pp. 809–852.
15. Pratt, S.J., Valencia, A.P., Le, G.K., Shah, S.B., and Lovering, R.M., *Front. Physiol*, 2015, vol. 6.
16. Rahimov, F. and Kunkel, L.M., *J. Cell Biol.*, 2013, vol. 201, pp. 499–510.
17. Cardenas, A.M., Gonzalez-Jamett, A.M., Cea, L.A., Bevilacqua, J.A., and Caviedes, P., *Exp. Neurol.*, 2016, vol. 283, pp. 246–254.
18. Allen, D.G., Whitehead, N.P., and Froehner, S.C., *Physiol Rev*, 2016, vol. 96, no. 1, pp. 253–305.
19. Kravtsova, V.V., Mikhailov, V.M., Sokolova, A.V., Mikhailova, E.V., Timonina, N.A., Nikol'skii, E.E., and Krivoi, I.I., *Dokl. Biol. Sci.*, 2011, vol. 441, no. 2, pp. 357–359.
20. Miles, M.T., Cottey, E., Cottey, A., Stefanski, C., and Carlson, C.G., *J. Neurosci.*, 2011, vol. 303, pp. 53–60.
21. Grounds, M.D., Terrill, J.R., Radley-Crabb, H.G., Robertson, T., Papadimitriou, J., Spuler, S., and Shavlakadze, T., *Am. J. Pathol.*, 2014, vol. 184, pp. 1668–1676.
22. Nagy, N., Nonneman, R.J., Llanga, T., Dial, C.F., Riddick, N.V., Hampton, T., Moy, S.S., Lehtimaki, K.K., Ahtoniemi, T., Puolivali, J., Windish, H., Albrecht, D., Richard, I., and Hirsch, M.L., *Physiol. Rev.*, 2017, vol. 5, no. 6, article e13173.
23. Heiny, J.A., Kravtsova, V.V., Mandel, F., Radzyukevich, T.L., Benziane, B., Prokofiev, A.V., Pedersen, S.E., Chibalin, A.V., and Krivoi, I.I., *J. Biol. Chem.*, 2010, vol. 285, pp. 28614–28626.
24. Matchkov, V.V. and Krivoi, I.I., *Front. Physiol.*, 2016, vol. 7, article 179.
25. Banks, G.B., Fuhrer, C., Adams, M.E., and Froehner, S.C., *J. Neurocytol.*, 2003, vol. 32, pp. 709–726.
26. Khan, M.M., Strack, S., Wild, F., Hanashima, A., Gasch, A., Brohm, K., Reischl, M., Carnio, S., Labeit, D., Sandri, M., Labeit, S., and Rudolf, R., *Autophagy*, 2014, vol. 10, pp. 123–136.
27. Pauly, M., Daussin, F., Burelle, Y., Li, T., Godin, R., Fauconnier, J., Koechlin-Ramonatxo, C., Hugon, G., Lacampagne, A., Coisy-Quivy, M., Liang, F., Hussain, S., Matecki, S., and Petrof, B.J., *Am. J. Pathol.*, 2012, vol. 181, pp. 583–592.
28. Bansal, D., Miyake, K., Vogel, S.S., Groh, S., Chen, C.C., Williamson, R., McNeil, P.L., and Campbell, K.P., *Nature*, 2003, vol. 423, pp. 168–172.
29. Han, R., Rader, E.P., Levy, J.R., Bansal, D., and Campbell, K.P., *Skelet. Muscle*, 2011, vol. 1, article 35.